MODELING OF A LUNENBURG LENS ANTENNA WITH THE INNER METALIC SPHERE

Dmitry V. Denisov,
Ural Federal University, Yekaterinburg, Russia;
Ural Technical Institute of Communications and Informatics, Ekaterinburg, Russia, ***denisov.dv55@gmail.com***

Vladislav Ya. Noskov,
Ural Federal University, Yekaterinburg, Russia,
denisov.dv55@gmail.com

Dmitry V. Kusaykin,
Ural Technical Institute of Communications and Informatics, Ekaterinburg, Russia, ***kusaykin@mail.ru***

DOI: 10.36724/2072-8735-2022-16-11-44-49

Manuscript received 05 October 2022;
Accepted 28 October 2022

This work was funded by the subsidy allocated the State Task No. 071-03-2022-001.

Keywords: *Luneberg lens, spherical antenna, electrodynamic modeling, diffraction, Green tensor function method*

One of the statutory principle of fifth generation mobile communications is the adaptive antenna system beam-forming technology that allow the radiation to be oriented to specific subscriber. Promising solution of the task can be using the passive antennas, which provide the direct beam-forming with no active component in the circuit, thus is low-cost. Lunenburg lens antenna is perspective solution of the task described above and allows the direct radiation to be formed in wide-angle range and keeps the required performance. Besides, it's slightly compact, so the antenna can be installed on various of city infrastructure elements, and the spherical form of device is advantage when the installation is performed on to the vehicles surface (train, car, aircraft, etc.) In the paper, the metallic sphere installation inside the spherical Lunenburg lens as a mean of attachment to constructions is described. The analysis results of the inner element impact to the antenna characteristics of the Lunenburg lens are provided. Analytical system model with the spherical conductor inside the antenna, which can also be used to calculate the presence of metallic particles impact to the average permittivity of the lens, is shown. The diffraction task is addressed by means of the Green's tensor functions application. The results of numerical modeling of the described antenna system using the Ansys Electronics Desktop (HFSS Design) are presented. Analytical and numerical calculations show that the limited-sized metallic sphere presence inside the lens does not significantly affect the focusing property of the device. The acquired formulas can be used in the future work to find the solution of the metallic element optimal radius approximation, using the neural networks as one of the mean to do it.

Information about authors:
Dmitry V. Denisov, *Candidate of Technical Sciences, Associate Professor of the Department of Information Technologies and Control Systems of the Institute of Radioelectronics and Information Technologies - RTF of the Ural Federal University, Yekaterinburg, Russia; Associate Professor of the Department of Information Systems and Technologies of the Ural Technical Institute of Communications and Informatics (branch) of the Siberian State University of Telecommunications and Informatics", Ekaterinburg, Russia*
Vladislav Ya. Noskov, *Doctor of Technical Sciences, Professor of the Department of Radio Electronics and Telecommunications of the Institute of Radio Electronics and Information Technologies - RTF Ural Federal University, Ekaterinburg, Russia*
Dmitry V. Kusaykin, *Candidate of Technical Sciences, Associate Professor of the Department of Multichannel Electrical Communication of the Ural Technical Institute of Communications and Informatics (branch) of the Siberian State University of Telecommunications and Informatics, Yekaterinburg, Russia*

Для цитирования:
Денисов Д.В., Носков В.Я., Кусайкин Д.В. Моделирование линзовой антенны Люнеберга с металлической сферой внутри // T-Comm: Телекоммуникации и транспорт. 2022. Том 16. №11. С. 44-49.

For citation:
Denisov D.V., Noskov V.Ya., Kusaykin D.V. (2022) Modeling of a Lunenburg lens antenna with the inner metalic sphere. *T-Comm*, vol. 16, no.11, pp. 44-49. (*in Russian*)

Introduction

Luneburg lens (LL) is a volumetric physical body capable of converting a spherical wave front into a flat one. This antenna can be used in the following applications: 5G wireless broadband communications, unmanned systems, automation and control systems, etc. [1,2]. Antennas based on spherical lenses have great potential also in radar and navigation. Luneburg lens can act as a highly directional antenna, but also as a diffuser in various radar scenarios. For example, LL is used as part of an air target E95M for testing air defense systems [3].

Today, there are many methods of LL manufacturing, especially using 3D printing technologies [4,5]. The material used in traditional 3D printers have the required electrophysical properties that necessary to create a Luneburg lens antenna. Due to the cheapness and wide prevalence of this type of plastic, the manufacture of antennas based on LL is no longer a difficult task. However, a sufficiently high print accuracy is required to synthesize a spherical lens. Therefore, the development of reliable electrodynamic models, preceding the manufacturing stage, is still an urgent task.

In addition, for a fairly large class of practical tasks, it can be useful to solve the problem of analyzing LL with a conductive sphere inside. Such problems are of practical interest both in the case of considering the issues of fastening a spherical lens to an object, and in considering the point of synthesizing a lens and selecting material parameters by adding inhomogeneities to the lens structure. Also, the obtained electrodynamic model can be used for calculating LL with a metal sphere, to solve the optimization problem when finding the optimal radius of attachment inside the sphere [6].

Setting the task

In order to create a LL with the required refractive index, an inhomogeneous dielectric must be used as the base material of the lens body. In this case, an stepwise and optimized approximation of the lens profile is possible. For stepwise approximation the entire interval of the spherical structure from its center to the surface (radius) is dividing into sections of equal width. Each section is a dielectric layer with certain parameters satisfying the R.K. Luneburg law. The dielectric constant value in the calculated lens model is taking from the midpoint of the layer. Such an approximation method is the simplest. When approximating the lens profile from the outside of the dielectric sphere, a virtual air layer (air gap) is attaching, which corresponds to the R.K. Luneburg law and allows to adjust the position of the irradiator relative to the lens body.

Table 1

Layer parameters at stepwise approximation of the lens profile

L	Layers radius	Layers dielectric constant ε'_l
1	0,5	1,75
2	0,333; 0,667	1,889; 1,556
3	0,25; 0,5; 0,75	1,938; 1,75; 1,438
4	0,2; 0,4; 0,6; 0,8	1,96; 1,84; 1,64; 1,36
5	0,167; 0,333; 0,5; 0,667; 0,833	1,972; 1,889; 1,75; 1,556; 1,306
6	0,143; 0,286; 0,429; 0,571; 0,714; 0,857	1,98; 1,918; 1,816; 1,673; 1,49; 1,265
7	0,125; 0,25; 0,375; 0,5; 0,625; 0,75; 0,875	1,984; 1,938; 1,859; 1,75; 1,609; 1,438; 1,234
8	0,111; 0,222; 0,333; 0,444; 0,556; 0,667; 0,778; 0,889	1,988; 1,951; 1,889; 1,802; 1,691; 1,556; 1,395; 1,21

**air gap between lens and irradiator. It's necessary according to Luneburg law.*

Table 1 shows the parameters of the layers that calculated according to the Luneburg law at stepwise approximation of the lens profile.

In order to bring the LL characteristics closer to the required ones, various optimization algorithms are also used, in particular, a quadrature approximation of stratification parameters to the required distribution law. For example - work of French authors [7]. Table 2 shows the electrophysical parameters of multilayer LL with optimized profile approximation.

Table 2

Layer parameters at optimized approximation of the lens profile

L	Layers radius	Layers dielectric constant ε'_l
1	0,82	1,67
2	0,63; 0,89	1,8; 1,4
3	0,53; 0,75; 0,93	1,86; 1,57; 1,28
4	0,47; 0,67; 0,82; 0,94	1,88; 1,67; 1,44; 1,22
5	0,43; 0,60; 0,74; 0,85; 0,95	1,91; 1,73; 1,55; 1,36; 1,18
6	0,39; 0,56; 0,68; 0,78; 0,88; 0,96	1,93; 1,77; 1,61; 1,46; 1,31; 1,16
7	0,37; 0,52; 0,63; 0,73; 0,82; 0,89; 0,97	1,93; 1,80; 1,67; 1,53; 1,40; 1,27; 1,13
8	0,34; 0,49; 0,59; 0,69; 0,77; 0,84; 0,91; 0,97	1,94; 1,82; 1,71; 1,59; 1,47; 1,35; 1,24; 1,12

Dielectric parameters can be changed to control its filling density during 3D printing on accordance with the parameters of the materials given in Tables 1, 2. By selecting the necessary values of the dielectric constant parameters, which varies from ~ 2 in the center to 1 on the surface, the spherical front of the wave can be transformed into a flat one on the shadow side of the lens, Figure 1.

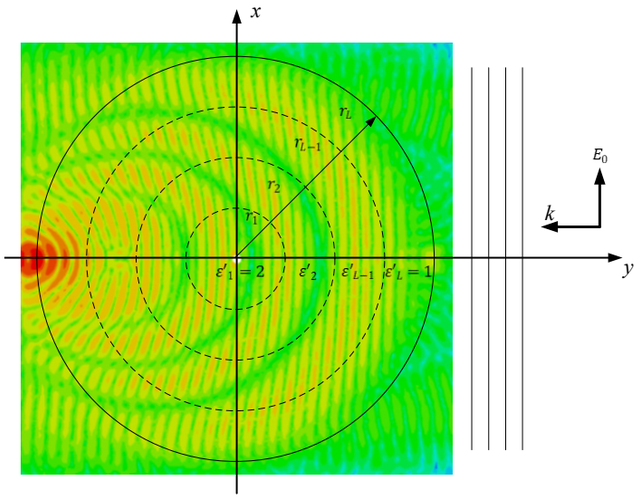

Fig. 1. Diffraction on multilayer Luneburg lens

In addition to 3D printing, there are other very original manufacturing options of the Luneburg lens. Most of them realize a stepwise approximation of the refractive index to Luneburg law. Specifically, the lens is realizing in the form of a multilayer material with different parameters of dielectric constant. Typically, the permittivity within each layer is constant and varies discretely from layer to layer.

Let's consider the developed model of a lens antenna with a metal sphere inside in the Ansys Electronics Desktop (HFSS Design) software package using parametric analysis. The body of the lens, as mentioned earlier, is built in the form of spheres with different dielectric constants. The model construction used an optimized approximation for the six-layer lens model. Dielectric constant and normalized radii of layers are given in Chart 2.

Figure 2 shows the geometry of the optimized separation of the lens into six layers. The number of layers is due to the fact that in this approach, with fewer layers, it is possible to achieve better antenna characteristics. In Figure 2, vector **k** indicates the direction of flat electromagnetic wave incidence on the sphere, $\mathbf{E_0}$ vector shows the plane of electric field oscillation.

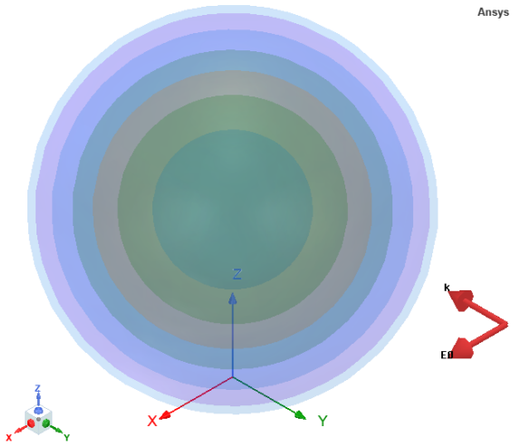

Fig. 2. Luneberg lens in the Ansys Electronics Desktop software package (HFSS Design) with optimized stratification of the six-layer model (the seventh layer is an air)

The spherical lens is irradiating by a flat electromagnetic wave of linear polarization. The lens model has a radius described by $r_L = 8\lambda$ (~24 cm). Frequency is about 10 Ghz. For comparison, radiation patterns of the lens were built without any redundant structures inside the sphere. Figure 3 shows the normalized radiation pattern by gain in two experimental planes. These results can be used as "reference" for further comparison with a modified model with a sphere of conductive material installed in the central part.

It should be noted that the authors in [6] considered the problem solution of calculating the lens with the central rod inside the sphere. At the same work, two cases were analyzed, which differ in the mutual orientation of the primary irradiator and the rod that acted as a supporting structure. These cases are shown in Figures 4a and 4b, where A and B are wide and narrow walls of the waveguide irradiator.

Figure 4a shows the geometry for the case where wide wall of the waveguide were parallel oriented to the metal rod. Similar composition for the case of orthogonal orientation are shown in Fig. 4b. Field structure and radiation patterns in both cases, in two experimental planes has been researched.

Figure 4b shows a model lens with a metal sphere inside. This model attractive from a practical point of view, for example, for those cases of LL calculation, when the central sphere can be made of a solid conductive material and acts as an element on which a fastening system of dielectric or metal guides are fixing.

The conductive sphere model discussed in this work can also be used to determine the effect of metal inclusions on the dielectric constant of the lens body.

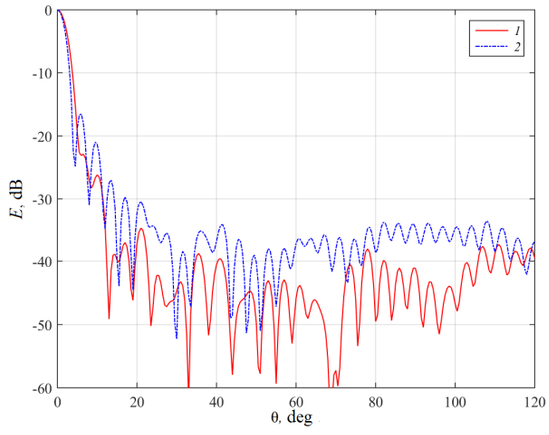

a)

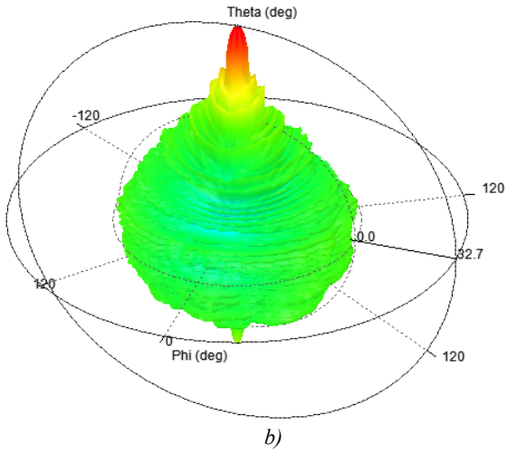

b)

Fig. 3. Graphs of the dependence of the amplitude multiplier $E(\theta)$ of the radiation pattern of a Luneberg lens without a central metal rod on angle θ sight (*a*) and the spatial view (*b*) of the radiation pattern calculated at (curve *1*) and at (curve *2*)

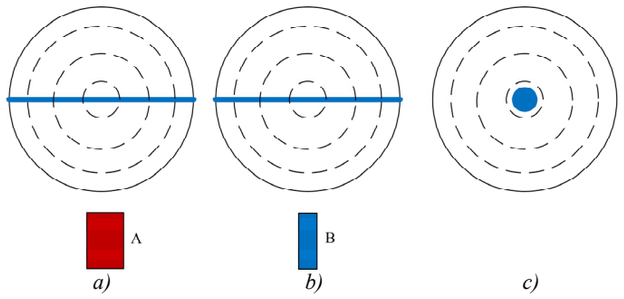

Fig. 4. The scheme of parallel (*a*) and orthogonal (*b*) orientation of the metal rod and the primary irradiator and the model (*c*) of the Luneberg lens with metal sphere inside

Solution of the Diffraction task

According to the problem mentioned in the previous chapter, one can see that the assessment of inner metallic sphere of the LL impact to the antenna characteristics, its sufficient to address the diffraction task. When finding the right solutions for the modeling tasks and designing of the lens with central element, the optimal positioning, appropriate size and possibly the number of spherical non-uformities are the questions required to find the solutions for. The optimal solution finder should be able to perform a rapid analysis of as great number of variables, which define the prototype geometry. Because of that, the highly accurate analytical formula seems to be useful to get. Green's tensor functions (GTF) applications reworked for the spherical layers analysis satisfies all the requirements to be the wanted formula. Here, the comparison of analytical solution and the finite-element model in the HFSS application is possible to calculate the described solution in terms of accuracy.

Analysis of the multi-layered spherical regions using the GTF application are well described in [8]. In this chapter calculation of the lens with the inner metallic element is to be shown. The aim is to obtain the optimal solution in terms of memory resources and calculation time (this solution would be consequently used in the optimiser, including the use neural network). Here, the diffraction task is wise to be described when applying the linear polarization. The task geometry is shown in Figure 5.

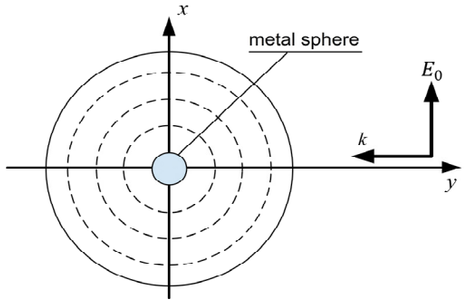

Fig. 5. Geometry of the problem of linear polarization wave diffraction on a multilayer sphere with a metallic element inside

The electromagnetic excitation using the remote source can be addressed with the GTF application and the methods that were described in [9]. The diffracted wave intensity field vector of electic fiend, when the linear polarization field is applied, in the far zone is acquired as (the formula is normalized ignoring the amplification multiplayer):

$$\vec{E}_\theta = \sum_{n=1}^{\infty} \frac{2n+1}{n(n+1)} \cdot (-1)^n \cdot \left(\tau_n(\theta) \cdot M_n - \pi_n(\theta) N_n\right) \quad (1)$$

$$\vec{E}_\varphi = \sum_{n=1}^{\infty} \frac{2n+1}{n(n+1)} \cdot (-1)^n \cdot \left(\pi_n(\theta) \cdot M_n - \tau_n(\theta) N_n\right) \quad (2)$$

where $\tau_n(\theta) = \frac{\partial P_n^1(\cos\theta)}{\partial\theta}$; $\pi_n(\theta) = \frac{P_n^1(\cos\theta)}{\sin\theta}$;

$P_n^1(\cos\theta)$ – Legendre function of the first kind - n-th order [9; 10]; $h_n(x)$, $j_n(x)$ – spherical Bessel – Ricatti functions [10]; $k_0 = 2\pi/\lambda$ – wave number;

$$M'_n = \frac{i\tilde{\tilde{Z}}_n(a) \cdot j_n(k_0 a) - j'_n(k_0 a)}{i\tilde{\tilde{Z}}_n(a) \cdot h_n(k_0 a) - h'_n(k_0 a)};$$

$$N'_n = \frac{i\tilde{\tilde{Y}}_n(a) \cdot j_n(k_0 a) - j'_n(k_0 a)}{i\tilde{\tilde{Y}}_n(a) \cdot h_n(k_0 a) - h'_n(k_0 a)}$$ – he coefficients of the medium calculated through oriented impedances and admittances directed respectively $\tilde{\tilde{Z}}_n(a)$, $\tilde{\tilde{Y}}_n(a)$ (a – radii of lens layers), which are determined by sequential recalculation from the outer boundary of the LL to the center through partial regions-layers according to the methodology described in [8]. The multilayered lense structure is defined with the environment coefficients M'_n and N'_n [8].

The expressions acquired allows to quickly approximate the metallic element impact on to the random-size LL antenna characteristics. Using the finite-elements method in the Ansys HFSS software would require significantly greater amount of time to address the task due to the fact that the increase of sphere radius leads to the multiple times geometry recalculation and the new grid model generation on the every single iteration of the sphere layers size change. Therefore, in this case the GFT based calculation time is wise. The analytical formula acquiring time and creating of the subprogram for the calculations in MATLAB decrease the numerical complexity in the Ansys Electronics Desktop (HFSS Design).

In order to shown the acquired formulas constructiveness and that the accurate assessment of the construction element impact on to the scattering diagram form (that is formed by the lens) using the formula is possible, let's have a look at the following cases. The first one is, using the Ansys HFSS, to calculate the scattering diagram on the lens with the inner spherical conductor. The second one is the scattering diagram obtain using the MATLAB by means of the expressions (1), (2). In the Fig. 6, the calculation results of are shown for different inner spherical conductor radius values of the LL.

Single geometry calculation using the analytical formulas in the MATLAB took a split of second. At the same time, the same geometry calculation (for the diffraction task) in the Ansys HFSS took 57 minute for every single variant, where the hardware equipment is as follows: the CPU is 8-core Intel® Xeon Intel(R) Xeon(R) Gold 6154 CPU @3.00GHz, the RAM amount is 47.5 GB. It's not the analytical and numerical methods comparison in terms of calculation performance.

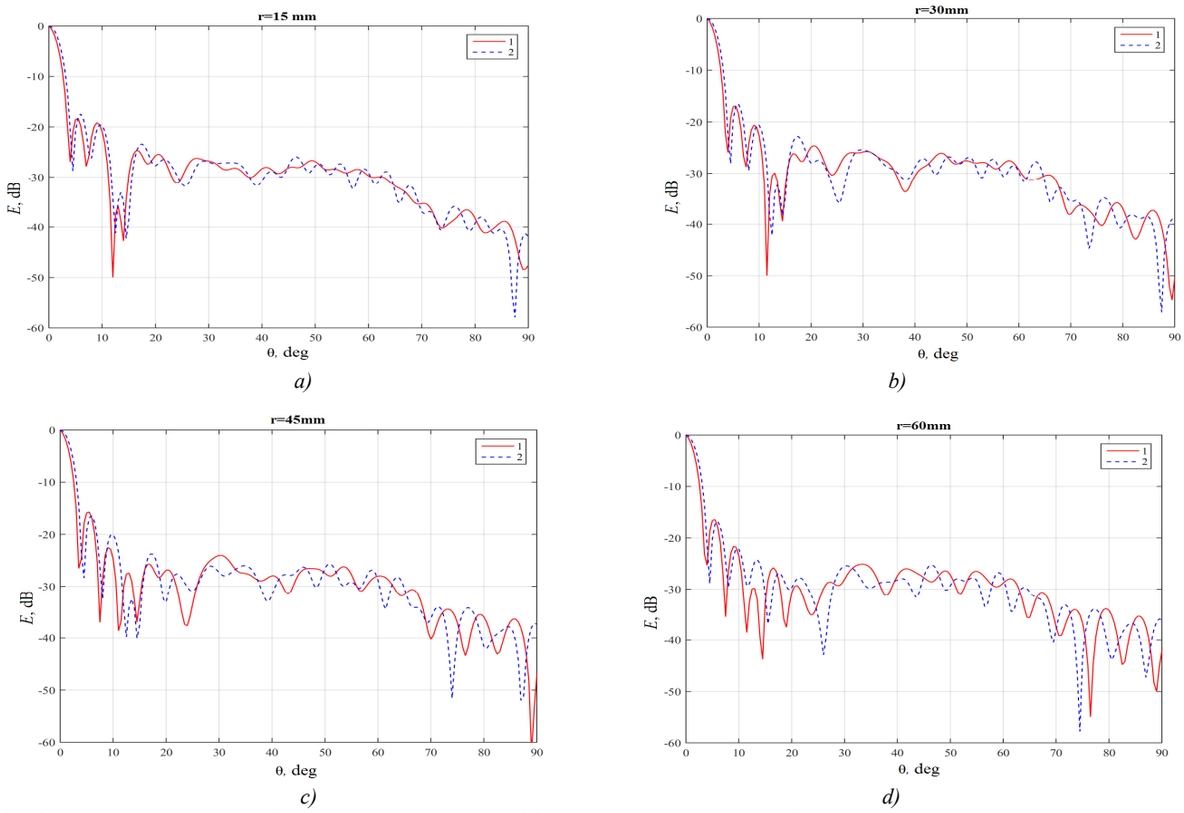

Fig. 6. Influence of the radius of the metal sphere inside the LL on its characteristics for different radii r of the metal sphere inside the lens: a) r = 15 ; b) r = 30 mm; c) r = 45 mm; d) r = 60 mm. The calculations were performed by the TGF method (curve 1) and in HFSS Design (curve 2)

More likely, it's the fact that the accuracy of the acquired analytical formula is good enough and that the formula can be used for further quick model optimization and searching for optimal positioning and the metallic element radius calculation as fast as possible. Having the described analytical formula allows to quickly estimate thousands of positioning and central lens element options and to find the optimal one. The above tasks can be addressed using the described expressions.

Conclusion

Presence of the metallic spherical element in the multilayered dielectric sphere might be not the best idea. However, in search for the options to install the lens on the objectives and to control the lens body permittivity coefficients leads to the need of the analysis of the conductor presence in the dielectric lens. In the paper, the calculation model in the special software and the analytical solution for calculation the lens with the inner spherical element were acquired. The results of analytical computations as well as of the modeling in the special software shown that the appropriate geometry of it leads to the lens focus to be satisfying the requirements.

The metallic element presence in the lens affects the equipment work regime and the lens characteristics. But for designing of the LL with all the advantages, including the field-performance, the use of such elements is reasonable.

Note that the propagation diagram irregularities due to the metallic element affection tends to be appropriate for the LL based antennas characteristics realization. Besided, the expressions gained using the GTF application is the way to address the optimization tasks in the fastest manner when checking for the optimal hypothesis around the variety of them using the parametric analysis and the neural networks.

References

1. Li Y., Ge L., Chen M., Zhang Z., Li Z., Wang J. (2019). Multi-Beam 3D Printed Luneburg Lens Fed by Magneto-Electric Dipole Antennas for Millimeter-Wave MIMO Applications. *IEEE Transactions on Antennas and Propagation*. Vol. 67, no. 5, pp. 2923-2933.

2. Modern millimeter wave Luneburg Lens. URL: https://lunewave.com/lenses (date of access: 15.08.2022)

3. Air target E95M. URL: http://enics.aero/products/e95 (date of access: 15.08.2022).

4. Bahr R. A., Adeyeye A. O., Van Rijs S., Tentzeris M. M. (2020). 3D-Printed Omnidirectional Luneburg Lens Retroreflectors for Low-Cost mm-Wave Positioning. *2020 IEEE International Conference on RFID*.

5. Kubach A., Shoykhetbrod A., Herschel R. (2017). 3D printed Luneburg lens for flexible beam steering at millimeter wave frequencies. *47th European Microwave Conference (EuMC)*, pp. 787-790.

6. Denisov D. V., Noskov V. Ya. (2022). The influence of a metal rod inside a spherical Luneberg lens on its characteristics. *Ural Radio Engineering Journal*. Vol. 6, no. 2, pp. 160-185.

7. Fuchs B. et al. (2007). Design Optimization of Multishell Luneburg Lenses. *IEEE Trans. Antennas Propag*. Vol. 55, no. 2, pp. 283-289.

8. Panchenko B.A. (2013). Scattering and absorption of electromagnetic waves by inhomogeneous spherical bodies. Moscow: Radio Engineering. 268 p. (in Russian)

9. Ishimaru A. (1978). Wave Propagation and Scattering in random Media. Academic Press. 572 p.

10. Abramovits M., Stigan I. (1979). Handbook of Special functions. Moscow: Science. 832 p. (in Russian)

МОДЕЛИРОВАНИЕ ЛИНЗОВОЙ АНТЕННЫ ЛЮНЕБЕРГА С МЕТАЛЛИЧЕСКОЙ СФЕРОЙ ВНУТРИ

Денисов Дмитрий Вадимович, *Уральский федеральный университет (УрФУ), г. Екатеринбург, Россия;*
Уральский технический институт связи и информатики (филиал) СИбГУТИ (УрТИСИ СИбГУТИ), г. Екатеринбург, Россия, ***denisov.dv55@gmail.com***
Носков Владислав Яковлевич, *Уральский федеральный университет, г. Екатеринбург, Россия,* ***noskov@oko-ek.ru***
Кусайкин Дмитрий Вячеславович, *Уральский технический институт связи и информатики (филиал) СИбГУТИ (УрТИСИ СИбГУТИ), г. Екатеринбург, Россия,* ***kusaykin@mail.ru***

Аннотация
Одним из неотъемлемых принципов систем мобильной связи пятого поколения является технология формирования адаптивной диаграммы направленности антенной системой, что позволяет направлять радиоизлучение к конкретному пользователю. Перспективным решением этой задачи могут выступать пассивные антенны, которые обеспечивают формирования луча в заданном направлении без использования активных компонентов и тем самым снижают затраты на энергоресурсы. Линзовая антенна Люнеберга является перспективным решением этой задачи и позволяет формировать направленное излучение в широком угловом диапазоне без ухудшения производительности. Кроме того, относительно компактные размеры антенны позволяют устанавливать ее на различных элементах городской инфраструктуры, а обтекаемая форма сферической антенны дает преимущества при установке на корпус транспортного средства (поезда, автомобили, самолеты и т. д.). В работе рассматривается вариант инсталляции металлической сферы внутрь сферической линзы Люнеберга как возможного средства крепления антенны на различных конструкциях. Представлены результаты анализа влияния этого конструктивного элемента на антенные характеристики линзы Люнеберга Рассмотрена аналитическая модель системы с проводящей сферой внутри линзы Люнеберга, которая может быть использована также для определения влияния металлических вкраплений на среднюю диэлектрическую проницаемость тела линзы. Дифракционная задача решается методом тензорных функций Грина. Представлены результаты компьютерного моделирования рассматриваемой антенной системы в программном пакете Ansys Electronics Desktop (HFSS Design). Результаты как аналитических расчетов, так и компьютерного моделирования показали, что наличие металлической сферы приемлемых геометрических размеров сохраняет фокусирующие свойства линзовой антенны Люнеберга. Полученные формулы могут быть использованы в дальнейшем для решения задачи поиска оптимального радиуса металлического элемента, в том числе с применением нейронных сетей.

Ключевые слова: *линза Люнеберга, сферическая антенна, электродинамическое моделирование, дифракция, метод тензорных функций Грина.*

Литература

1. *Li, Y., Ge, L., Chen, M., Zhang, Z., Li, Z., Wang, J.* Multi-Beam 3D Printed Luneburg Lens Fed by Magneto-Electric Dipole Antennas for Millimeter-Wave MIMO Applications // IEEE Transactions on Antennas and Propagation, 2019. Vol. 67, no. 5, pp. 2923-2933.
2. Modern millimeter wave Luneburg Lens. URL: https://lunewave.com/lenses (date of access: 15.08.2022)
3. Air target E95M. URL: http://enics.aero/products/e95 (date of access: 15.08.2022)
4. *Bahr R. A., Adeyeye A. O., Van Rijs S., Tentzeris M. M.* 3D-Printed Omnidirectional Luneburg Lens Retroreflectors for Low-Cost mm-Wave Positioning // 2020 IEEE International Conference on RFID. 2020.
5. *Kubach A., Shoykhetbrod A., Herschel R.* 3D printed Luneburg lens for flexible beam steering at millimeter wave frequencies // 47th European Microwave Conference (EuMC). 2017, pp. 787-790.
6. *Денисов Д. В., Носков В. Я.* Влияние металлического стержня внутри сферической линзы Люнеберга на ее характеристики. Уральский радиотехнический журнал, 2022. Вып. 6, № 2. С. 160-185.
7. *Fuchs B.* et al. Design Optimization of Multishell Luneburg Lenses // IEEE Trans. Antennas Propag, 2007. Vol. 55, no. 2. P. 283-289.
8. Panchenko B. A. Scattering and absorption of electromagnetic waves by inhomogeneous spherical bodies. Moscow: Radio Engineering, 2013. P. 268. (in Russian)
9. *Ishimaru A.* Wave Propagation and Scattering in random Media. Academic Press, 1978. 572 p.
10. *Абрамовиц М., Стиган И.* Справочник специальных функций. Москва: Наука, 1979. 832 с.

Информация об авторах:
Денисов Дмитрий Вадимович, *к.т.н., доцент, доцент кафедры информационных технологий и систем управления Института радиоэлектроники и информационных технологий Уральского федерального университета (УрФУ); доцент кафедры информационных систем и технологий Уральского технического института связи и информатики (филиал) СИбГУТИ (УрТИСИ СИбГУТИ), г. Екатеринбург, Россия*
Носков Владислав Яковлевич, *д.т.н., профессор, профессор кафедры радиоэлектроники и телекоммуникаций Института радиоэлектроники и информационных технологий Уральского федерального университета, г. Екатеринбург, Россия*
Кусайкин Дмитрий Вячеславович, *к.т.н., доцент, доцент кафедры многоканальной электрической связи Уральского технического института связи и информатики (филиал) СИбГУТИ (УрТИСИ СИбГУТИ), г. Екатеринбург, Россия*